

PREPARED FOR SUBMISSION TO JCAP

Extracting parity-violating gravitational waves from projected tidal force tensor in three dimensions

Teppei Okumura^{a,b} and Misao Sasaki^{b,c,d}

^aInstitute of Astronomy and Astrophysics, Academia Sinica, No. 1, Section 4, Roosevelt Road, Taipei 10617, Taiwan

^bKavli Institute for the Physics and Mathematics of the Universe (WPI), UTIAS, The University of Tokyo, Kashiwa, Chiba 277-8583, Japan

^cCenter for Gravitational Physics, Yukawa Institute for Theoretical Physics, Kyoto University, Kyoto 606-8502, Japan

^dLeung Center for Cosmology and Particle Astrophysics, National Taiwan University, Taipei 10617, Taiwan

E-mail: tokumura@asiaa.sinica.edu.tw, misao.sasaki@ipmu.jp

Abstract. Gravitational waves (GWs) may be produced by various mechanisms in the early universe. In particular, if parity is violated, it may lead to the production of parity-violating GWs. In this paper, we focus on GWs on the scale of the large-scale structure. Since GWs induce tidal deformations of the shape of galaxies, one can extract such GW signals by observing images of galaxies in galaxy surveys. Conventionally the detection of such signals is discussed by considering the three-dimensional power spectra of the E/B -modes. Here, we develop a complementary new technique to estimate the contribution of GWs to the tidal force tensor field projected on the celestial sphere, which is a directly observable quantity. We introduce two two-dimensional vector fields constructed by taking the divergence and curl of the projected tidal field in three dimensions. Their auto-correlation functions naturally contain contributions of the scalar-type tidal field. However, we find that the divergence of the curl of the projected tidal field, which is a pseudo-scalar quantity, is free from the scalar contribution and thus enables us to extract GW signals. We also find that we can detect parity-violating signals in the GWs by observing the nonzero cross-correlation between the divergence of the projected tidal field and the curl of it. It roughly corresponds to measuring the cross-power spectrum of E and B -modes, but these are complementary to each other in the sense that our estimator can be naturally defined locally in position space. Finally we present expressions of the correlation functions in the form of Fourier integrals, and discuss the properties of the kernels specific to the GW case, which we call the overlap reduction function, borrowing the terminology used in the pulsar timing array experiments.

Keywords: galaxy surveys, gravity, inflation, large-scale structure, primordial gravitational waves (theory)

ArXiv ePrint: [2405.04210](https://arxiv.org/abs/2405.04210)

Contents

1	Introduction	1
2	Gravitational waves in tidal force field	3
2.1	Polarizations of gravitational waves	4
2.2	Power spectra of tidal force field	5
3	Projected tidal force field in three dimensions	6
3.1	Power spectra of projected tidal force field	8
3.2	Power spectra of divergence and curl of projected tidal force field	8
3.3	Correlation functions and overlap reduction functions	10
4	Conclusions and discussion	13
A	Relation to E/B-mode decomposition	15
B	Power spectra of projected field before subtracting the trace	16
C	Derivation of power spectra of projected tidal force field	16
C.1	Power spectra of scalar tidal field	16
C.2	Power spectra of tensor tidal field	17

1 Introduction

Detecting cosmological gravitational wave (GW) backgrounds has become one of the hot topics in cosmology. On very large scales, $\sim \text{Gpc}$, the primordial GWs originating from the vacuum fluctuations during inflation [1] can be probed by measuring the B -mode signal in the polarization of the cosmic microwave background (CMB) [2, 3]. On very small scales, $\sim 10^8 - 10^{13} \text{cm}$ ($\sim 10^{-3} - 10^2 \text{Hz}$), interferometric gravitational wave detectors, either ground-based or space-based, may be able to detect a cosmological GW background in the near future [4–7]. Recently, several pulsar time array (PTA) collaborations announced the detection of a GW background on pc scales ($\sim 10^{-8} \text{Hz}$) [8–10]. On the other hand, a vast range of wavelengths corresponding to the large-scale structure of the universe, $\sim 1 - 100 \text{Mpc}$, has not been explored well, though a number of theoretical considerations have been given, as GWs on these scales may be encoded in the large-scale structure as dynamical and projection effects on the galaxy clustering and weak gravitational lensing by GWs [11–20].

In all these studies, one of the intriguing questions asked is if there exists parity violation in a GW background. There is a growing interest in finding parity asymmetry in cosmological observations, e.g., birefringence [21–23], galaxy spins [24–28], and galaxy/CMB four-point correlation functions [29–32]. If parity is violated in the early universe, it may source the tensor perturbation of the metric, leading to the production of parity-violating GWs [33–44]. It was pointed out that astrometry can be used to detect parity violation on pc scales [45]. In this paper, we focus on GWs with wavelengths $\sim 10 - 100 \text{Mpc}$.

The galaxy shapes are intrinsically aligned with the surrounding large-scale dark matter distribution, known as intrinsic alignment (IA) [46–49]. Orientations of the major axis of

galaxies were shown to be linearly aligned with the surrounding tidal field in both simulations and observations [50–52], which led to the possibility of IA of galaxy shapes being a powerful probe of various cosmological effects [53–57]. Recent studies have developed accurate theoretical models for statistics of galaxy IA in full three dimensions [58–65]. Thus, the cosmological information encoded in the IA of galaxies can be maximized by measuring galaxy shapes in galaxy redshift surveys [66–72].

Ref. [73] proposed that GWs directly affect shapes of galaxies as the instantaneous response effect, similarly to the scalar tidal field case above. Ref. [74] extended the work and investigated the possible upper limit on the parity-violating GWs, but they still considered angular statistics. Ref. [75] utilized a separate universe technique and confirmed using N -body simulations the ansatz between the effects of GWs and scalar tidal field on galaxy shapes proposed by Ref. [73]. Refs. [75–77] computed the auto-power spectra of the E - and B -modes as well as their cross-power spectrum in three dimensions. The latter can be particularly used to search for the parity-violation signals. These three-dimensional power spectra are observables in galaxy redshift surveys, since the projected shapes of galaxies on the celestial sphere are measured via imaging observations and the distances to them are via spectroscopic observations [58, 66, 78, 79]. This is opposed to the power spectra of CMB which provides angular (two-dimensional) modes. Furthermore, a galaxy survey targets different scales, and thus it is complimentary to the CMB surveys. One difficulty of measuring the effect of GWs on galaxy shapes in this way is that it requires a large survey volume because the E -/ B -modes are quantities defined in Fourier space hence global in real space. Thus, it is not straightforward to estimate the effects of GWs locally in a small region of the universe.

In this paper, we develop and present a new technique to extract gravitational wave signals from the projected tidal force field in three dimensions. We introduce two two-dimensional vector fields constructed by taking the divergence and curl of the projected tidal field. We show that taking their auto-correlations enables us to extract signals of the GWs. Furthermore, we show that cross-correlating the divergence of the projected tidal field and the curl of it allows us to extract parity-violating signals in the GWs. These new estimators are complementary to the power spectra of the E - and B -mode fields in the sense that our estimator can be naturally defined locally in position space. To be more specific, the similarity is that both the EB decomposition used in the CMB community [3] and the method developed here focus on the tensor field projected on the celestial sphere. On the other hand, the main difference is that while the EB decomposition is defined in terms of spherical harmonics, hence globally defined from the real space point of view, our method involves only spatial derivative operations to single out the tensor components, hence is defined locally in space. It is thus straightforward to present the expressions of the correlation functions. Our formalism is admittedly quite fundamental in the sense that it assumes an ideal observational situation. Nevertheless, we hope it will eventually lead to a unique method for detecting an extremely low frequency GW background, with the corresponding wavelengths of 10 - 100 Mpc, that may or may not contain parity-violating components.

The structure of the paper is as follows. In section 2, we give a review on the decomposition of GWs into the polarizations and power spectra. In section 3, we present the formalism for extracting the GW power spectrum from the projected tidal force field in three dimensions. Our conclusions are given in section 4. Appendix A provides the relation between our formalism and the E -/ B -mode decomposition. In Appendix B we present the power spectra of the projected tidal field before the trace part is subtracted. In Appendix C, we show

detailed derivations for the formulas of the power spectra given in section 3.

Throughout this paper, we use the Einstein summation convention, i.e., the summation is assumed when the same letters appear in the upper and lower indices simultaneously.

2 Gravitational waves in tidal force field

Let us start by defining GWs in the cosmological background. We define GWs by the transverse and traceless tensor perturbation, $h_{ij}^{\text{TT}}(\eta, \mathbf{x})$, of the metric. Together with the scalar perturbation, the perturbed metric is expressed as

$$ds^2 = -a^2(\eta) \left([1 + 2\Psi(\eta, \mathbf{x})] d\eta^2 + \{ [1 - 2\Psi(\eta, \mathbf{x})] \delta_{ij} + h_{ij}^{\text{TT}}(\eta, \mathbf{x}) \} dx^i dx^j \right), \quad (2.1)$$

where η is the conformal time, $\Psi(\eta, \mathbf{x})$ the Newton potential, $a(\eta)$ the scale factor and δ_{ij} is Kronecker's delta, and we assumed that the anisotropic stress is negligible. In the following, we omit the superscript "TT" from h_{ij}^{TT} .

The tidal force is described by the geodesic deviation equation, with the force given in terms of the Riemann tensor. At linear order in cosmological perturbation theory, it is expressed in terms of the perturbative components δR^k_{0j0} . For the metric (2.1), it is given by

$$\delta R^k_{0j0}(\eta, \mathbf{x}) = \left[\Psi''(\eta, \mathbf{x}) + 2\mathcal{H}(\eta)\Psi'(\eta, \mathbf{x}) + \frac{1}{3}\nabla^2\Psi(\eta, \mathbf{x}) \right] \delta_j^k + \delta^{ki} F_{ij}(\eta, \mathbf{x}), \quad (2.2)$$

where $\mathcal{H} \equiv aH$ is the conformal Hubble parameter and $F_{ij}(\eta, \mathbf{x})$ is the traceless part that defines the tidal field and given by

$$F_{ij}(\eta, \mathbf{x}) \equiv \left(\partial_i \partial_j - \frac{1}{3} \delta_{ij} \nabla^2 \right) \Psi(\eta, \mathbf{x}) - \frac{1}{2} [h''_{ij}(\eta, \mathbf{x}) + \mathcal{H}(\eta) h'_{ij}(\eta, \mathbf{x})]. \quad (2.3)$$

Below we focus on the traceless components. To evaluate the cosmological tidal effect, it is convenient to introduce a dimensionless tidal field, defined by

$$f_{ij}(\eta, \mathbf{x}) \equiv \frac{F_{ij}(\eta, \mathbf{x})}{4\pi G \bar{\rho}(\eta) a^2} = s_{ij}(\eta, \mathbf{x}) + t_{ij}(\eta, \mathbf{x}), \quad (2.4)$$

where

$$s_{ij}(\eta, \mathbf{x}) \equiv \frac{1}{4\pi G \bar{\rho} a^2} \left(\partial_i \partial_j - \frac{1}{3} \delta_{ij} \nabla^2 \right) \Psi(\eta, \mathbf{x}) = \left(\frac{\partial_i \partial_j}{\nabla^2} - \frac{1}{3} \delta_{ij} \right) \delta_m(\eta, \mathbf{x}), \quad (2.5)$$

$$t_{ij}(\eta, \mathbf{x}) \equiv -\frac{1}{8\pi G \bar{\rho} a^2} [h''_{ij}(\eta, \mathbf{x}) + \mathcal{H}(\eta) h'_{ij}(\eta, \mathbf{x})], \quad (2.6)$$

with $\bar{\rho}$ being the background energy density and $\delta_m(\eta, \mathbf{x})$ the matter density contrast. Note that we have assumed the scale of our interest to be small enough so that the Newtonian approximation is valid. In the real Universe, this should be valid on scales $\lesssim 500$ Mpc.

Due to the scalar potential term, it is hard to extract the tensor part, GWs, from observations because it is subdominant, as estimated below. One of the goals of this paper is to formulate a method to extract the tensor part from the tidal field based solely on observables. As we intend to develop the basic formalism, in this paper we assume an ideal situation for observation and ignore all possible observational errors.

2.1 Polarizations of gravitational waves

We consider the tidal field in Fourier space, $X_{ij}(\eta, \mathbf{k}) = \int d^3x X_{ij}(\eta, \mathbf{x})e^{-i\mathbf{k}\cdot\mathbf{x}}$ ($X = \{s, t \text{ or } h\}$). The scalar contribution, $s_{ij}(\eta, \mathbf{k})$, is given by $s_{ij}(\eta, \mathbf{k}) = \left(\hat{k}_i\hat{k}_j - (1/3)\delta_{ij}\right)\delta_m(\eta, \mathbf{k})$. We decompose GWs in Fourier space into the right-handed (R) and left-handed (L) polarizations (e.g., [80, 81]),

$$h_{ij}(\eta, \mathbf{k}) = e_{ij}^{(R)}(\hat{\mathbf{k}})h_{(R)}(\eta, \mathbf{k}) + e_{ij}^{(L)}(\hat{\mathbf{k}})h_{(L)}(\eta, \mathbf{k}), \quad (2.7)$$

$$e_{ij}^{(R,L)}(\hat{\mathbf{k}}) = \frac{1}{\sqrt{2}} \left(e_{ij}^{(+)}(\hat{\mathbf{k}}) \pm i e_{ij}^{(\times)}(\hat{\mathbf{k}}) \right), \quad (2.8)$$

where hat denotes a unit vector, for instance $\hat{\mathbf{k}} = \mathbf{k}/k$, and $e_{ij}^{(+)} = \frac{1}{\sqrt{2}}(e_i^{(1)}e_j^{(1)} - e_i^{(2)}e_j^{(2)})$ and $e_{ij}^{(\times)} = \frac{1}{\sqrt{2}}(e_i^{(1)}e_j^{(2)} + e_i^{(2)}e_j^{(1)})$, with $\mathbf{e}^{(1)}$ and $\mathbf{e}^{(2)}$ being arbitrary orthonormal vectors spanning two-dimensional space orthogonal to $\hat{\mathbf{k}}$. We assume the set $(\mathbf{e}^{(1)}, \mathbf{e}^{(2)}, \hat{\mathbf{k}})$ forms a right-handed Cartesian basis. All the polarization tensors are defined to be orthonormal, $e_{ij}^{(p)}e_{(p')}^{ij} = \delta_{p'}^p$ for $p, p' = \{+, \times\}$, and $e_{ij}^{(p)}\bar{e}_{(p')}^{ij} = \delta_{p'}^p$ for $p, p' = \{R, L\}$, where a bar stands for the complex conjugate.

In passing, we note that it is useful to express the Fourier component of the dimensionless tidal field t_{ij} given by (2.6) in terms of h_{ij} . Assuming $k \gg \mathcal{H}$, we have $t_{ij} \propto h_{ij}'' = -k^2 h_{ij}$. Hence

$$t_{ij}(\eta, \mathbf{k}) = \frac{k^2}{3\mathcal{H}^2} h_{ij}(\eta, \mathbf{k}), \quad (2.9)$$

where we have used the background Friedmann equation for a spatially flat universe, $8\pi G\bar{\rho}a^2 = 3\mathcal{H}^2$. Noting that $s_{ij} = O(\delta_m)$, the tensor contribution can be comparable to the scalar one only when $h_{ij} \sim (\mathcal{H}^2/k^2)\delta_m$. On 10 Mpc scale, which is approximately the scale of our interest, we have $\delta_m = O(1)$. This means we need $h_{ij} \sim 10^{-4}$ to dominate over the scalar contribution on that scale, which seems practically impossible to attain. Conversely, we need a method to cleanly separate out the scalar contribution if we are to detect the tensor part in the tidal field.

We now define the symmetric curl field of a given tensor field X_{ij} [82] by putting the asterisk on the left-hand side of the symbol, $*X_{ij}$, as

$$*X_{ij}(\eta, \mathbf{x}) \equiv \frac{1}{2} \left(\epsilon_i^{mn} \partial_m X_{nj} + \epsilon_j^{mn} \partial_m X_{ni} \right), \quad (2.10)$$

where $\epsilon_i^{mn} = \delta_{ij}\epsilon^{jmn}$ and ϵ^{jmn} is the totally anti-symmetric unit tensor with $\epsilon^{123} = 1$. By taking the spatial derivative of Eq. (2.7), we get

$$\partial_m h_{nj}(\eta, \mathbf{x}) = \int \frac{d^3k}{(2\pi)^3} i k_m \left[e_{nj}^{(R)}(\hat{\mathbf{k}})h_{(R)}(\eta, \mathbf{k}) + e_{nj}^{(L)}(\hat{\mathbf{k}})h_{(L)}(\eta, \mathbf{k}) \right] e^{i\mathbf{k}\cdot\mathbf{x}}. \quad (2.11)$$

Then the curl of the tidal field reads

$$*h_{ij}(\eta, \mathbf{x}) = \int \frac{d^3k}{(2\pi)^3} *h_{ij}(\eta, \mathbf{k})e^{i\mathbf{k}\cdot\mathbf{x}}, \quad (2.12)$$

where

$$*h_{ij}(\eta, \mathbf{k}) = k \left[e_{ij}^{(R)}(\hat{\mathbf{k}})h_{(R)}(\eta, \mathbf{k}) - e_{ij}^{(L)}(\hat{\mathbf{k}})h_{(L)}(\eta, \mathbf{k}) \right]. \quad (2.13)$$

In the above we used the identities, $i \epsilon_i^{mn} k_m e_{nj}^{(R,L)} = \pm k e_{ij}^{(R,L)}$ [83]. Note that apart from the flip of sign of the L-mode, $*h_{ij}$ is essentially equivalent to the spatial derivative of h_{ij} . Since the curl of the scalar component is identically zero, the above equation states that if we detect the non-zero curl component of the tidal force field at large scales where linearized theory give an accurate prediction, it provides a direct evidence of the signal of gravitational waves.

2.2 Power spectra of tidal force field

The auto-power spectra of the gravitational waves h_{ij} and their curl field $*h_{ij}$ are given by

$$\begin{aligned} \langle h^{ij}(\eta, \mathbf{k}) h_{ij}(\eta', \mathbf{k}') \rangle &= k^{-2} \langle *h^{ij}(\eta, \mathbf{k}) *h_{ij}(\eta', \mathbf{k}') \rangle \\ &= (2\pi)^3 \delta_D(\mathbf{k} + \mathbf{k}') P_h(\eta, \eta', k), \end{aligned} \quad (2.14)$$

where $P_h(\eta, \eta', k)$ is the temporal auto correlation power spectrum that reduces to the standard power spectrum at equal time $\eta = \eta'$. The (dimensionless) tidal field f_{ij} consists of the scalar and tensor components as given by (2.4). We mention again that since the scalar component is curl-free, $*s^{ij} = 0$, measuring $*f_{ij}$ enables us to extract the signal of GWs t_{ij} out of the tidal field f_{ij} .

The power spectra of each polarization is defined similarly as

$$\begin{aligned} \langle h^{(\lambda)}(\eta, \mathbf{k}) h_{(\lambda)}(\eta', \mathbf{k}') \rangle &= k^{-2} \langle *h^{(\lambda)}(\eta, \mathbf{k}) *h_{(\lambda)}(\eta', \mathbf{k}') \rangle \\ &= (2\pi)^3 \delta_D(\mathbf{k} + \mathbf{k}') P_{(\lambda)}(\eta, \eta', k), \end{aligned} \quad (2.15)$$

where $\lambda = \{R, L\}$ and $P_{(R)} = P_{(L)} = P_h/2$ for unpolarized GWs. The cross-power spectra of the curl field $*h_{ij}$ and the original field h_{ij} are given by

$$\langle *h^{ij}(\eta, \mathbf{k}) h_{ij}(\eta', \mathbf{k}') \rangle = (2\pi)^3 \delta_D(\mathbf{k} + \mathbf{k}') k \chi(\eta, \eta', k) P_h(\eta, \eta', k), \quad (2.16)$$

$$\langle *h^{(\lambda)}(\eta, \mathbf{k}) h_{(\lambda)}(\eta', \mathbf{k}') \rangle = (2\pi)^3 \delta_D(\mathbf{k} + \mathbf{k}') k \chi(\eta, \eta', k) P_{(\lambda)}(\eta, \eta', k), \quad (2.17)$$

where we introduced the chiral parameter $\chi(\eta, k)$ to quantify parity violation in GWs,

$$\chi(\eta, \eta', k) \equiv \frac{P_{(R)}(\eta, \eta', k) - P_{(L)}(\eta, \eta', k)}{P_h(\eta, \eta', k)}. \quad (2.18)$$

Namely, taking the cross correlation enables us to extract a signal of parity violation [42].

Let us now turn to the general properties of the power spectrum. First we formally write the total tensor field, $h_{(\lambda)}^{(\text{total})}$, as a sum of the contributions of primordial GWs, denoted by $h_{(\lambda)}$, and that generated by a source $S_{(\lambda)}$ at some epoch in the early universe, denoted by $H_{(\lambda)}$. Thus $h_{(\lambda)}^{(\text{total})} = h_{(\lambda)} + H_{(\lambda)}$, where $\square h_{(\lambda)} = 0$ and $\square H_{(\lambda)} = S_{(\lambda)}$. To compute $H_{(\lambda)}$, we assume the wavenumbers are much larger than the Hubble parameter at the time of generation, $k \gg \mathcal{H}$, which is reasonable from causality. Let us introduce $g_{(\lambda)}(\eta, \mathbf{k})$ by $H_{(\lambda)}(\eta, \mathbf{k}) = g_{(\lambda)}(\eta, \mathbf{k})/a(\eta)$. The green function at the $k\eta \gg 1$ limit is given by (e.g., [84])

$$G(\eta - \eta') = \Theta(\eta - \eta') \sin[k(\eta - \eta')]/k, \quad (2.19)$$

where $\Theta(\eta)$ is the step function. Assuming that GWs are generated during an epoch, $\eta_i < \eta < \eta_i + \Delta\eta$, the solution $g_{(\lambda)}$ is given by

$$g_{(\lambda)}(\eta, \mathbf{k}) = \int_{\eta_i}^{\eta_i + \Delta\eta} d\eta' \frac{\sin[k(\eta - \eta')]}{k} a(\eta') S_{(\lambda)}(\eta', \mathbf{k}), \quad (2.20)$$

where $S_{(\lambda)}(\eta, \mathbf{k})$ is the Fourier component of $S_{(\lambda)}(\eta, \mathbf{x})$. Regardless of the form of $S_{(\lambda)}$, $g_{(\lambda)}$ has the form of $g_{(\lambda)}(\eta, \mathbf{k}) = g_0(\eta, \mathbf{k}) \cos(k\eta + \phi_{\mathbf{k}})$ at $\eta > \eta_i + \Delta\eta$. Taking the product with itself and ensemble average, the $\phi_{\mathbf{k}}$ term vanishes and we obtain

$$P_{(\lambda)}^S(\eta, \eta', k) = \frac{\langle |g_0(k)|^2 \rangle}{a(\eta)a(\eta')} \cos[k(\eta - \eta')], \quad (2.21)$$

where the superscript S indicates its the spectrum of GWs generated by a source. As for the primordial GWs, the corresponding power spectrum can be expressed as

$$P_{(\lambda)}^P(\eta, \eta', k) = T(\eta, k)T(\eta', k)P_{(\lambda)}^{\text{ini}}(k), \quad (2.22)$$

where the superscript P denotes its primordial and $T(\eta, k)$ is the transfer function of GWs. For $k \gg \mathcal{H}$, we have $T(\eta, k) \simeq \cos[k\eta + \varphi_k]/a(\eta)$ where φ_k is not random now but determined by the history of the equation of state of the early universe (for example, if the universe were radiation-dominated for the entire history, $\varphi_k = 0$). Nevertheless, taking into account the effect of inhomogeneities in the universe, it is expected that the phase ϕ_k will acquire an uncontrollable random noise after the wave has propagated over a distance much larger than the wavelength [85, 86]. Therefore, for the modes of our interest, i.e., $k\eta \gg 1$, the power spectrum $P_{(\lambda)}^P(\eta, \eta', k)$ reduces to the form same as $P_{(\lambda)}^S(\eta, \eta', k)$ in (2.21).

Thus the two-point correlation function can be generically expressed as

$$\xi_{(\lambda)}(\eta, \eta', \mathbf{x} - \mathbf{x}') = \int \frac{k^2 dk}{(2\pi)^3} \int d\Omega_k P_{(\lambda)}(\eta, \eta', k) e^{i\mathbf{k} \cdot (\mathbf{x} - \mathbf{x}')}, \quad (2.23)$$

where

$$\begin{aligned} P_{(\lambda)}(\eta, \eta', k) &= P_{(\lambda)}^P(\eta, \eta', k) + P_{(\lambda)}^S(\eta, \eta', k) \\ &= \frac{a_0^2}{a(\eta)a(\eta')} \cos[k(\eta - \eta')] P_{(\lambda)}(k). \end{aligned} \quad (2.24)$$

The $\cos[k(\eta - \eta')]/(a(\eta)a(\eta'))$ dependence of the two-point function is the characteristic feature of cosmological GWs, either primordial or generated by a transitional source, in contrast to the case of the two-point function of the density contrast, $\langle \delta_m(k, \eta)\delta_m(k, \eta') \rangle \propto a(\eta)a(\eta')$. Finally, we note that because the time dependence of $P_{(\lambda)}$ is independent of the polarization λ , the chiral parameter defined in (2.18) reduces to a function of only k , $\chi = \chi(k)$.

3 Projected tidal force field in three dimensions

In the previous section, we saw how the two-point correlation functions of GWs behave and how the parity-violating component shows up. However, they cannot be constructed solely from observables because we can observe only the past lightcone, which is a three-dimensional surface, while the quantities discussed in the previous section assume that we can observe h_{ij} in the whole four-dimensional spacetime. In this section, to overcome this difficulty, we develop a formalism that uses only the observable quantities. Galaxy morphologies, such as the spins and ellipticities of galaxies, are projected onto the celestial plane in observation. Analogously, we deal only with the tensor perturbation projected on the celestial sphere, with the line of sight direction identified as the time toward the past.

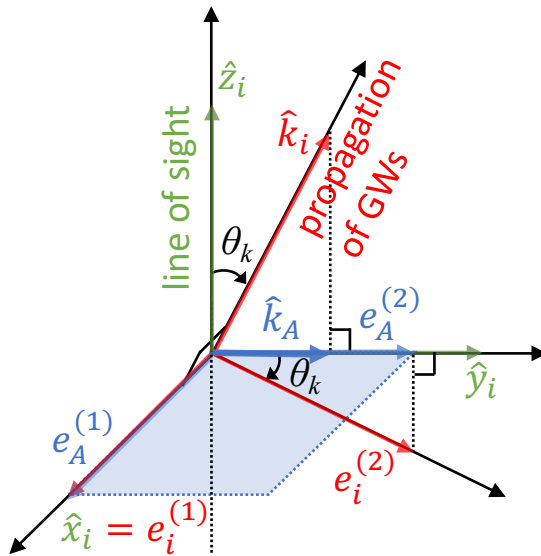


Figure 1. Illustration of the coordinates adopted in the text. The direction of $\hat{\mathbf{z}}$ is the observer’s line of sight, and the orthonormal vectors $\hat{\mathbf{x}}, \hat{\mathbf{y}}$ and $\hat{\mathbf{z}}$ form a right-handed Cartesian basis. The direction of propagation of a GW is specified by $\mathbf{e}^{(3)} = \hat{\mathbf{k}}$, tilted from the line of sight by an angle θ_k , and $\mathbf{e}^{(1)}, \mathbf{e}^{(2)}$ and $\mathbf{e}^{(3)}$ form another right-handed Cartesian basis. Here $\mathbf{e}^{(1)}$ and $\hat{\mathbf{x}}$ are chosen to coincide with each other, $\mathbf{e}^{(1)} = \hat{\mathbf{x}}$. The components of the basis vectors projected onto the celestial sphere are denoted by capital letters such as $e_A^{(1)}$.

For this purpose, in this section we need to be more specific about the coordinates we adopt. We choose the direction along observer’s line of sight as $\hat{\mathbf{z}}$, where the hat means it is a unit vector. Since the direction of propagation of GWs is arbitrary, we set the angle between the direction and the line of sight to θ_k and the directional cosine, $\hat{\mathbf{k}} \cdot \hat{\mathbf{z}} = \cos \theta_k \equiv \mu_k$. The polarization tensor lies on the surface perpendicular to $\hat{\mathbf{k}}$, spanned by $\mathbf{e}^{(1)}$ and $\mathbf{e}^{(2)}$. The celestial sphere is locally spanned by two orthonormal basis vectors, say, $\hat{\mathbf{x}}'$ and $\hat{\mathbf{y}}'$. In this coordinate system, the components of $\hat{\mathbf{k}}$ may be expressed as $\hat{\mathbf{k}} = (\sin \theta_k \cos \phi_k, \sin \theta_k \sin \phi_k, \cos \theta_k)$. For convenience, one can rotate the axes by $\pi/2 - \phi_k$ to make the new basis vector $\hat{\mathbf{x}}$ coincide with $\mathbf{e}^{(1)}$. Namely, we choose the x -axis such that $\hat{\mathbf{x}} = \mathbf{e}^{(1)}$. Then the components, $\mathbf{e}^{(1)}$, $\mathbf{e}^{(2)}$ and $\hat{\mathbf{k}}$, respectively, have in the Cartesian coordinates,

$$e_i^{(1)} = (1, 0, 0), \quad e_i^{(2)} = (0, \cos \theta_k, -\sin \theta_k), \quad \hat{k}_i = (0, \sin \theta_k, \cos \theta_k). \quad (3.1)$$

Then the components of the basis vectors defined/projected on the celestial sphere in two dimensions are given by

$$e_A^{(1)} = \hat{x}_A = (1, 0), \quad e_A^{(2)} = \hat{y}_A \cos \theta_k = (0, \cos \theta_k), \quad \hat{k}_A = \hat{y}_A \sin \theta_k = (0, \sin \theta_k). \quad (3.2)$$

where the capital Latin indices denote quantities on the two-dimensional celestial sphere. Figure 1 is an illustration of the coordinate system.

Note that the tidal force field is characterized by the second time derivative, $a^{-1}(ah'_{ij})'$, rather than h_{ij} itself, as shown in Eq. (2.2). For the scale of our interest, $k^2 \gg \mathcal{H}^2$, we can approximate it by h''_{ij} . Thus, the power spectra relevant to observations are those of the

second time derivative of GWs, and for instance the power spectrum of given fields X and Y , $\langle X^{ij}Y_{ij} \rangle = (2\pi)^3 \delta_D(\mathbf{k}+\mathbf{k}') P_{XY}(k)$, should be replaced by $\langle \tilde{X}^{ij}\tilde{Y}_{ij} \rangle = (2\pi)^3 \delta_D(\mathbf{k}+\mathbf{k}') \tilde{P}_{XY}(k)$, where $\tilde{X} = X''$ and $\tilde{P}_{XY} = k^4 P_{XY}(k)$. In the following, however, we consider h_{ij} itself. This means all the resulting formulas should be multiplied by k^4 when they are to be considered as the tidal force field.

3.1 Power spectra of projected tidal force field

Since only the tidal field projected on the sphere perpendicular to the line of sight is observable, we consider the projected field of GWs, $h_{AB}(\eta, \mathbf{x})$ in real space or $h_{AB}(\eta, \mathbf{k})$ in Fourier space. Note that the vectors \mathbf{x} and \mathbf{k} are in three dimensions. We assume that we can measure the three-dimensional positions of galaxies via, say, measuring redshifts in spectroscopic galaxy surveys. The main purpose of this section is to derive formulas that can be used to identify the GW contribution in the tidal field solely from the projected field h_{AB} .

Let us first note that the tidal force field relevant to observables is a traceless part in two dimensions,

$$f_{AB}^T(\eta, \mathbf{x}) = s_{AB}^T(\eta, \mathbf{x}) + t_{AB}^T(\eta, \mathbf{x}), \quad (3.3)$$

where a quantity X with the superscript T stands for $X_{AB}^T = X_{AB} - \frac{1}{2}\delta_{AB}X^C_C$. In appendix B we present the power spectra of the projected field before the trace part is subtracted.

It is straightforward to compute the power spectrum of the projected scalar tidal field. The resulting spectrum is obtained as

$$\langle s^{T,AB}(\eta, \mathbf{k}) s_{AB}^T(\eta', \mathbf{k}') \rangle = \frac{1}{2} (2\pi)^3 \delta_D(\mathbf{k} + \mathbf{k}') k^4 (1 - \mu_k^2)^2 P_\psi(\eta, \eta', k), \quad (3.4)$$

where $\mu_k = \hat{\mathbf{k}} \cdot \hat{\mathbf{z}}$ and $\langle \psi(\eta, \mathbf{k}) \psi(\eta', \mathbf{k}') \rangle = (2\pi)^3 \delta_D(\mathbf{k} + \mathbf{k}') P_\psi(\eta, \eta', k)$ with $\psi(\eta, \mathbf{k}) \equiv \Psi(\eta, \mathbf{k})/4\pi G\bar{\rho}a^2$. Let us then compute the power spectra of the projected GWs. The GW power spectrum is obtained as

$$\langle h^{T,AB}(\eta, \mathbf{k}) h_{AB}^T(\eta', \mathbf{k}') \rangle = \frac{1}{8} (2\pi)^3 \delta_D(\mathbf{k} + \mathbf{k}') (1 + 6\mu_k^2 + \mu_k^4) P_h(\eta, \eta', k). \quad (3.5)$$

Taking the average over μ_k leads to the monopole component, $\frac{2}{5}P_h(\eta, \eta', k)$. However, it is hard to extract the GW signals via these expressions as the scalar potential term, $\langle s^{T,AB}(\eta, \mathbf{k}) s_{AB}^T(\eta', \mathbf{k}') \rangle$, dominates the signal, which prevent us to extract out the GW contribution directly. In practice the scalar contribution is the one commonly measured in the analysis of intrinsic alignment of galaxy shapes (see discussion in section 4 below). In appendix A we show how they are related to the power spectra of E- and B-modes. The derivations of these equations are given in Appendix C.

3.2 Power spectra of divergence and curl of projected tidal force field

We now consider to isolate the GW contribution from the observed projected tidal force field. We introduce the two-dimensional vector fields, X_A and $*X_A$, constructed respectively by taking the divergence and curl of the original projected field $X_{AB}(\eta, \mathbf{x})$ ($X = \{s, t \text{ (or } h)\}$) as

$$X_A(\eta, \mathbf{x}) \equiv \partial^B X_{BA}(\eta, \mathbf{x}), \quad *X_A(\eta, \mathbf{x}) \equiv \epsilon^{BC} \partial_B X_{CA}(\eta, \mathbf{x}), \quad (3.6)$$

where ϵ^{BC} is the Levi-Civita symbol defined in two dimensions. Similarly, the two-dimensional vector fields after subtracting the trace part, X_A^T and $*X_A^T$, are obtained from $X_{AB}^T(\eta, \mathbf{x})$ as

$$X_A^T(\eta, \mathbf{x}) \equiv \partial^B X_{BA}^T(\eta, \mathbf{x}), \quad *X_A^T(\eta, \mathbf{x}) \equiv \epsilon^{BC} \partial_B X_{CA}^T(\eta, \mathbf{x}). \quad (3.7)$$

Note that ${}^*s_A = 0$ but ${}^*s_A^T \neq 0$. That is, unlike the three-dimensional case, the curl of the scalar component does not vanish unless one can accurately identify the trace part of s_{AB} . Taking the curl of the projected tidal force field therefore does not immediately remove the scalar contribution.

In Fourier space, the divergence and curl of the field f_{AB} are expressed as

$$f_A^T(\eta, \mathbf{k}) = i k^B f_{BA}^T(\eta, \mathbf{k}) = f_A(\eta, \mathbf{k}) + \frac{i}{2} k_A [t^z(\eta, \mathbf{k}) - k^C k_C \psi(\eta, \mathbf{k})], \quad (3.8)$$

$${}^*f_A^T(\eta, \mathbf{k}) = i k_B \epsilon^{BC} f_{CA}^T(\eta, \mathbf{k}) = {}^*f_A(\eta, \mathbf{k}) + \frac{i}{2} k_B \epsilon^B_A [t^z(\eta, \mathbf{k}) + k^C k_C \psi(\eta, \mathbf{k})]. \quad (3.9)$$

Nonzero power spectra for the divergence and curl of the projected scalar tidal field with or without the trace part subtracted have the same form, and are given by

$$\begin{aligned} \langle s^{T,A}(\eta, \mathbf{k}) s_A^T(\eta', \mathbf{k}') \rangle &= \langle {}^*s^{T,A}(\eta, \mathbf{k}) {}^*s_A^T(\eta', \mathbf{k}') \rangle \\ &= \frac{1}{4} (2\pi)^3 \delta_D(\mathbf{k} + \mathbf{k}') k^6 (1 - \mu_k^2)^3 P_\psi(\eta, \eta', k). \end{aligned} \quad (3.10)$$

They are also related to the power spectrum of the original projected scalar tidal field via a simple relation, $\langle s^{T,A}(\eta, \mathbf{k}) s_A^T(\eta', \mathbf{k}') \rangle = \frac{1}{2} k^2 (1 - \mu_k^2) \langle s^{T,AB}(\eta, \mathbf{k}) s_{AB}^T(\eta', \mathbf{k}') \rangle$. Below we intend to formulate two-point statistics of ${}^*t_A^T$, or equivalently ${}^*h_A^T$ as given by (2.9).

We can also derive the auto-power spectra for the divergence and curl of the traceless projected field. They are given by

$$\begin{aligned} \langle h^{T,A}(\eta, \mathbf{k}) h_A^T(\eta', \mathbf{k}') \rangle &= \langle {}^*h^{T,A}(\eta, \mathbf{k}) {}^*h_A^T(\eta', \mathbf{k}') \rangle \\ &= \frac{1}{16} (2\pi)^3 \delta_D(\mathbf{k} + \mathbf{k}') k^2 (1 - \mu_k^2) (1 + 6\mu_k^2 + \mu_k^4) P_h(\eta, \eta', k) \\ &= \frac{1}{2} k^2 (1 - \mu_k^2) \langle h^{T,AB}(\eta, \mathbf{k}) h_{AB}^T(\eta', \mathbf{k}') \rangle. \end{aligned} \quad (3.11)$$

By taking an average over angle μ_k , we may extract out the monopole component $\propto k^2 P_h(k)$. We can similarly obtain the quadrupole and hexadecapole moments. As mentioned above and similarly to equation (3.5), this contribution of GWs cannot be separated from that of the scalar potential term, $\langle s^{T,A}(\eta, \mathbf{k}) s_A^T(\eta', \mathbf{k}') \rangle$.

Since ${}^*s^{T,A} \propto \epsilon^{BA} \partial_B \psi$, we cannot isolate the GW signals by computing the auto correlation of the curl of the projected field. However, if we take the divergence of the projected field, the scalar component vanishes, $\partial_A {}^*s^{T,A} \equiv 0$. Thus, similarly to the full three-dimensional case, Eq. (2.14), we can extract out GWs from the projected tidal force field. Specifically, let us introduce the symbols,

$${}^*X^T(\eta, \mathbf{x}) = \partial^A {}^*X_A^T(\eta, \mathbf{x}), \quad {}^*X^T(\eta, \mathbf{k}) = i k^A {}^*X_A^T(\eta, \mathbf{k}). \quad (3.12)$$

By setting $X^T = h^T$, we obtain a direct probe of a GW signal. The power spectrum is given by

$$\langle {}^*h^T(\eta, \mathbf{k}) {}^*h^T(\eta', \mathbf{k}') \rangle = \frac{1}{4} (2\pi)^3 \delta_D(\mathbf{k} + \mathbf{k}') k^4 \mu_k^2 (1 - \mu_k^2)^2 P_h(\eta, \eta', k). \quad (3.13)$$

We emphasize that measuring the above requires only the observable quantities.

Now we consider the possibility to detect a signal of parity violation from the projected two-dimensional field of GWs, similar to the three-dimensional case given by Eq. (2.16). Our

basic assumption is that we can only measure the projected tidal field, but in three dimensions. In section 2.2 we have seen that the parity violation appears in the cross correlation of h_{ij} and ${}^*h_{ij}$. Our goal here is to derive a similar equation in terms of the projected field. A straightforward choice for this purpose is to consider the cross-correlation of h_A^T and ${}^*h_A^T$. We obtain

$$\langle {}^*h^{T,A}(\eta, \mathbf{k})h_A^T(\eta', \mathbf{k}') \rangle = \frac{i}{4}(2\pi)^3\delta_D(\mathbf{k} + \mathbf{k}')k^2\mu_k(1 - \mu_k^4)\chi(k)P_h(\eta, \eta', k). \quad (3.14)$$

This is one of the main results of this paper. This power spectrum becomes nonzero if and only if parity is violated and the effect appears in the odd multipole moments. This cross power corresponds to the cross power spectrum of the E - and B -modes. The relation to the E/B decomposition is discussed in Appendix A. The derivations of the expressions for all the power spectra for the scalar and tensor tidal fields in this subsection are provided in Appendices C.1 and C.2, respectively.

3.3 Correlation functions and overlap reduction functions

Here we perform the Fourier transform of the power spectra of the projected tidal force field with the trace part subtracted, derived in the previous subsection, and present the expressions of the corresponding correlation functions. The two-point function of the projected field h_{AB}^T is given by

$$\langle h^{T,AB}(\eta, \mathbf{x})h_{AB}^T(\eta', \mathbf{x}') \rangle = \int \frac{k^2 dk}{(2\pi)^3} \int d\Omega_k P_{hh}^T(\eta, \eta', \mathbf{k}) e^{i\mathbf{k}\cdot(\mathbf{x}-\mathbf{x}')}, \quad (3.15)$$

where P_{hh}^T is the power spectrum derived in the previous subsection,

$$P_{hh}^T(\eta, \eta', \mathbf{k}) = \frac{1}{8}(1 + 6\mu_k^2 + \mu_k^4)P_h(\eta, \eta', k). \quad (3.16)$$

To evaluate the two-point function, let us first specify the four vectors of the two points, x'^α and x^α , as

$$x'^\alpha = (\eta', x'^i) = (\eta_0 - r', 0, 0, r'), \quad (3.17)$$

$$x^\alpha = (\eta, x^i) = (\eta_0 - r, r \sin \theta \cos \phi, r \sin \theta \sin \phi, r \cos \theta), \quad (3.18)$$

where the observer's position is set to the origin, and $r = |\mathbf{x}|$ and $x^i = r\hat{x}^i$. Also, we set the components of the four wavevector k_α as

$$k_\alpha = (-k, k \sin \theta_k \cos \phi_k, k \sin \theta_k \sin \phi_k, k \cos \theta_k), \quad (3.19)$$

where $k = |\mathbf{k}|$. Here we consider a more general coordinate system than that in Fig. 1 in which the wavevector can point to arbitrary directions. We can then perform the ϕ_k integral in equation (3.15) to obtain

$$\int_0^{2\pi} \frac{d\phi_k}{2\pi} e^{i\mathbf{k}\cdot(\mathbf{x}-\mathbf{x}')} = J_0(kr \sin \theta \sin \theta_k) e^{ik(r' - r \cos \theta) \cos \theta_k}, \quad (3.20)$$

where J_0 is the 0-th order Bessel function.

To proceed further, we introduce $\Delta\eta \equiv \eta - \eta' = r' - r$. Eventually, the correlation function is expressed as

$$\langle h^{T,AB}(\eta, \mathbf{x}) h_{AB}^T(\eta', \mathbf{x}') \rangle = \frac{a_0^2}{a(\eta)a(\eta')} \int \frac{k^4 dk}{2\pi^2} P_h(k) \Gamma_{hh}(kr, k\Delta\eta, \theta). \quad (3.21)$$

Here, let us call the kernel Γ_{hh} an overlap reduction function (ORF), borrowing the terminology used in the context of pulsar timing arrays [87–89] where the kernel for GWs is called the Hellings-Downs curve [90]. In our case, it is given by

$$\Gamma_{hh}(kr, k\Delta\eta, \theta) = \cos(k\Delta\eta) \int_0^1 d\mu_k \frac{1 + 6\mu_k^2 + \mu_k^4}{8} J_0 \left(A\sqrt{1 - \mu_k^2} \right) \cos(B\mu_k), \quad (3.22)$$

where

$$A(kr, \theta) = kr \sin \theta, \quad B(kr, k\Delta\eta, \theta) = -k\Delta\eta + 2kr \sin^2(\theta/2). \quad (3.23)$$

We can derive the similar expression for the correlation function of the projected scalar tidal field,

$$\langle s^{T,AB}(\eta, \mathbf{x}) s_{AB}^T(\eta', \mathbf{x}') \rangle = \int \frac{k^4 dk}{2\pi^2} P_\psi(\eta, \eta', k) \Gamma_{ss}(kr, k\Delta\eta, \theta), \quad (3.24)$$

where the scalar ORF is given by

$$\Gamma_{ss}(kr, k\Delta\eta, \theta) = \int_0^1 d\mu_k \frac{(1 - \mu_k^2)^2}{2} J_0 \left(A\sqrt{1 - \mu_k^2} \right) \cos(B\mu_k). \quad (3.25)$$

As clear from the above two expressions, we expect that Γ_{hh} and Γ_{ss} show different θ - and $\Delta\eta$ -dependences, which we confirm later. This property may be useful in identifying the GW contribution from the noisy data that contain the scalar contribution.

Finally, let us present the correlation functions that contain only the GW contribution,

$$\langle {}^*h^T(\eta, \mathbf{x}) {}^*h^T(\eta', \mathbf{x}') \rangle = \frac{a_0^2}{a(\eta)a(\eta')} \int \frac{k^2 dk}{2\pi^2} P_h(k) \Gamma_{*h*h}(kx, k\Delta\eta, \theta), \quad (3.26)$$

$$\langle {}^*h^{T,A}(\eta, \mathbf{x}) h_A^T(\eta', \mathbf{x}') \rangle = \frac{a_0^2}{a(\eta)a(\eta')} \int \frac{k^2 dk}{2\pi^2} P_h(k) \chi(k) \Gamma_{*hh}(kx, k\Delta\eta, \theta), \quad (3.27)$$

where

$$\Gamma_{*h*h}(kx, k\Delta\eta, \theta) = \cos(k\Delta\eta) \int_0^1 d\mu_k \frac{\mu_k^2(1 - \mu_k^2)^2}{4} J_0 \left(A\sqrt{1 - \mu_k^2} \right) \cos(B\mu_k), \quad (3.28)$$

$$\Gamma_{*hh}(kx, k\Delta\eta, \theta) = \cos(k\Delta\eta) \int_0^1 d\mu_k \frac{\mu_k(1 - \mu_k^4)}{4} J_0 \left(A\sqrt{1 - \mu_k^2} \right) \sin(B\mu_k). \quad (3.29)$$

Once again, we note that Γ_{*h*h} , is the important quantity to extract parity-violating signals from the projected tidal field in real space. Since the cross-power spectrum is purely imaginary as seen in eq. (3.14), the ORF has $\sin(B\mu_k)$ in the integrand rather than $\cos(B\mu_k)$.

Figure 2 shows the ORFs for the correlation functions of the projected scalar (Γ_{ss}) and tensor (Γ_{hh}) tidal fields. Both functions become almost constant for varying θ at $kr \ll 1$ and fixed $k\Delta\eta$. At $kr \gg 1$, both functions start to oscillate due to the term,

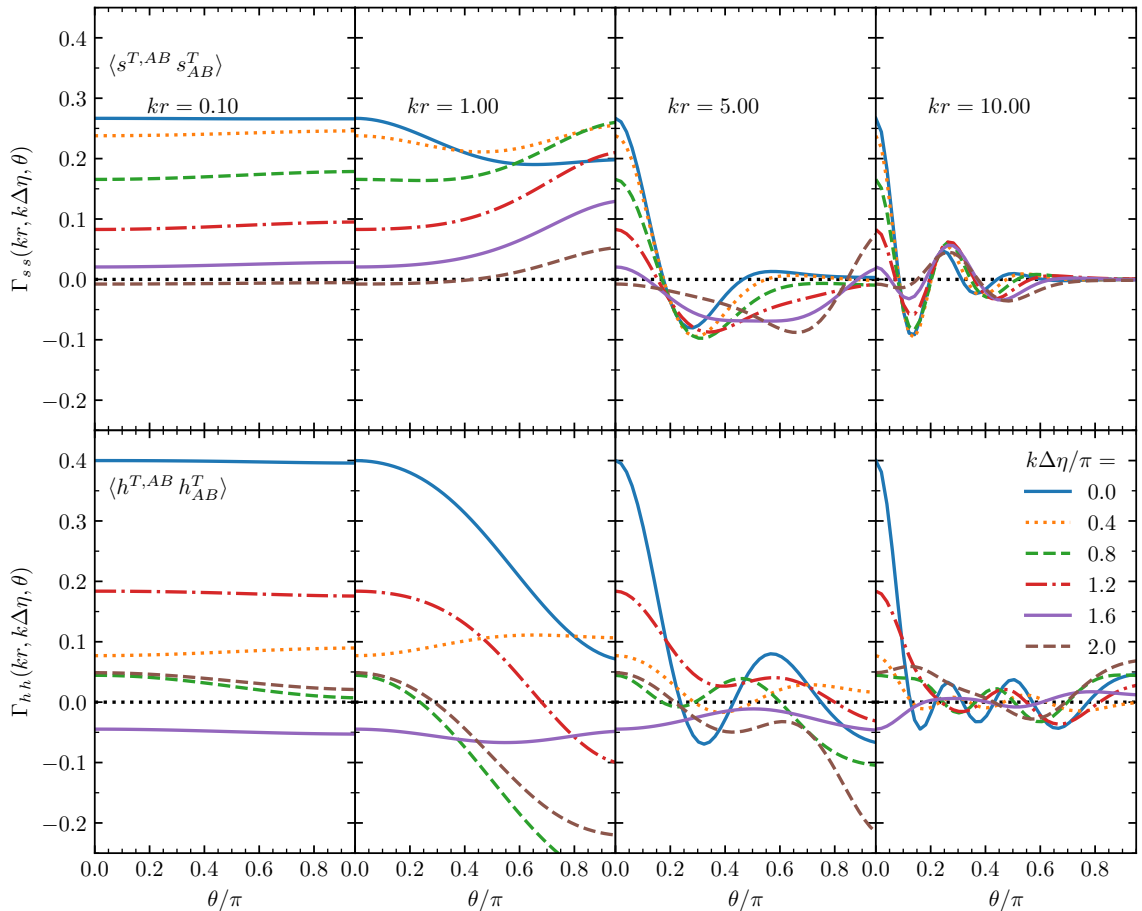


Figure 2. The kernels (ORFs) in the integrands of the correlation functions for the scalar and tensor (GW) components of the projected tidal force field. The upper and lower rows show the ORFs for the scalar and tensor tidal fields, respectively. Different columns show the results for several different values of kr and different lines show those for different values of $k\Delta\eta = k(r' - r)$.

$\cos(B\mu_k) = \cos([-k\Delta\eta + 2kr \sin^2(\theta/2)]\mu_k)$. However, the ORF for the tensor tidal field has the characteristic oscillatory feature due to the factor $\cos(k\Delta\eta)$ because GWs propagate through spacetime, while that of the scalar tidal field does not. Thus, given an accurate galaxy redshift survey data set, we confirm that it is in principle possible to distinguish the contributions of the scalar and tensor tidal forces by template matching applied to the projected tidal field data in three dimensions.

Figure 3 shows the two ORFs for signals of GWs that can be directly extracted from observation. The upper row shows the result for the divergence of the curl of the projected tidal tensor field, Γ_{*h^*h} . Although the overall behavior of the kernel Γ_{*h^*h} is similar to that of Γ_{hh} , GW signals can be directly extracted from this quantity since $*s \equiv 0$. The lower row shows the ORF for parity violation signals of the tidal tensor field. It becomes zero at the $\theta = 0$ and $k\Delta\eta = 0$ limit, unlike the ORFs for the other auto-correlations (see, e.g., Ref.[37] for a similar trend).

Finally let us comment on the corresponding quantities defined in terms of the dimen-

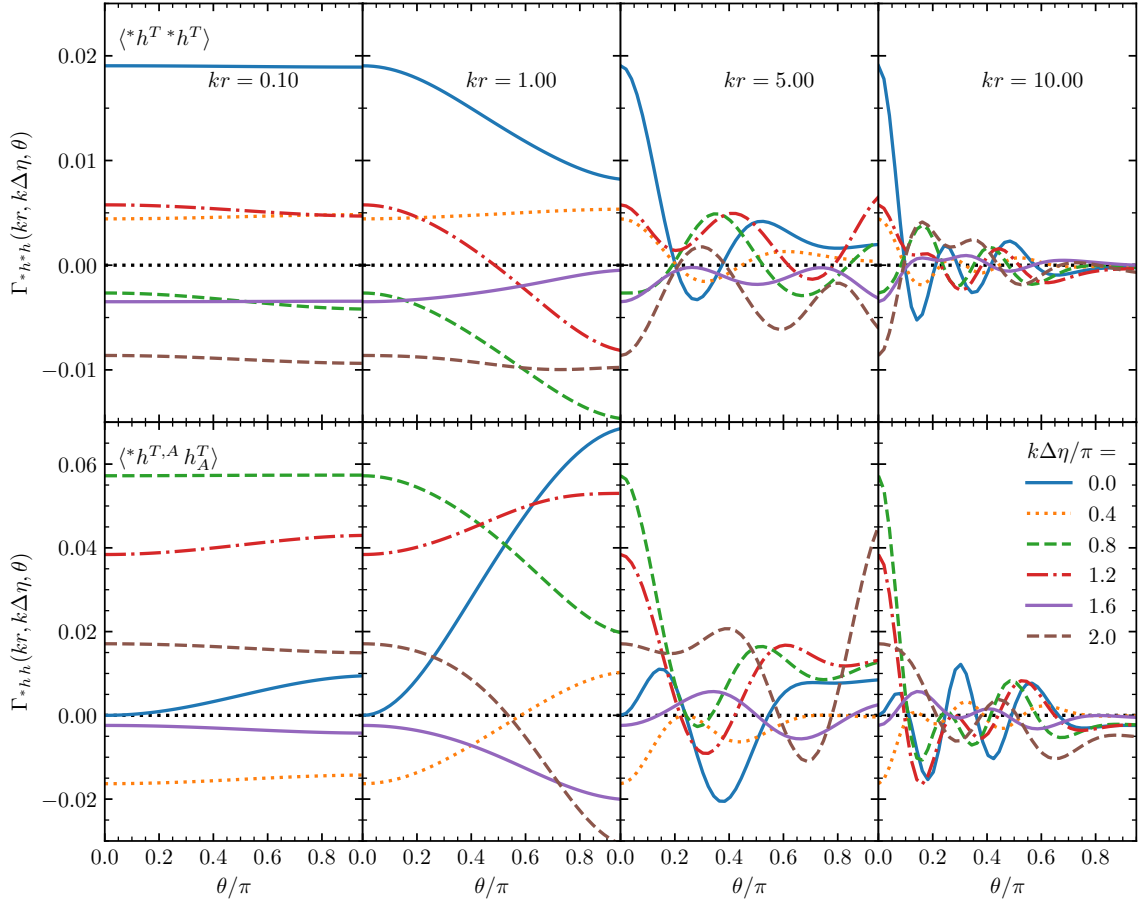


Figure 3. Similar with figure 2 but for the auto-correlation function of the curl of the projected GWs (*upper row*) and its cross-correlation function with the divergence (*lower row*).

tionless tidal force field $t_{ij} \approx (k^2/3\mathcal{H}^2)h_{ij}$ instead of h_{ij} . Under the assumption that the universe is matter-dominated, we have $k^2/\mathcal{H}^2 \propto a(\eta)$. Hence this scale factor dependence cancels the $1/a(\eta)$ dependence of h_{ij} . This means that the amplitude of t_{ij} at the epoch of matter-radiation equality is equal to that of t_{ij} at any later times. In the actual universe, because of the dark energy contribution, this estimate is no longer accurate, but it nevertheless gives a fairly good estimate of the amplitude of t_{ij} .

4 Conclusions and discussion

Gravitational waves (GWs) are known to be imprinted into the tidal force field as tensor perturbations. It can be estimated by defining E-/B-modes and computing their power spectra. In this paper, we have developed a new technique to estimate the contribution of GWs in the projected tidal field. We introduced two two-dimensional vector fields in three dimensions constructed by taking the divergence and curl of the projected tidal field, denoted by h^A and $*h^A$, respectively. The auto-power spectra naturally contain contributions of the scalar-type tidal field. We found that further taking the divergence of $*h^A$, which is a pseudo-scalar quantity, enable us to remove the scalar contribution and thus to single out

the GW contribution. The cross-correlation between h^A and $*h^A$ is free from the scalar tidal contribution, and it is non-vanishing only if parity is violated. Thus signals of parity violation in the GW background can be extracted from this cross-correlation, if any. It roughly corresponds to measuring the cross-power spectrum of E and B -modes, but these are complementary to each other in the sense that our estimator can be naturally defined locally in position space. We expressed the two-point functions in the Fourier integral form where the integrand is divided to the two factors; the power spectrum and the kernel, which we called the overlap reduction function (ORF), following the terminology used in pulsar timing array data analysis. We pointed out that the difference between the ORF of the tensor component and that of the scalar component may be used to identify the GW contribution in the tidal force field.

We now discuss how the tidal force tensor studied above is imprinted into the observed galaxy shapes. The scalar tidal field is known to be linearly related to the galaxy shape, known as the linear alignment model [47, 49, 52, 58]. Under this model the observed projected halo shape field, γ_{AB}^S , is related to the projected tidal field s_{AB} linearly as $\gamma_{AB}^S(\eta, \mathbf{k}) = b_K^S(\eta)s_{AB}(\eta, \mathbf{k})$. We can observe only the trace-free part of the projected galaxy shape. Here thus we omit the superscript T from all the quantities for clarity. The coefficient b_K^S is called the linear shape bias for the scalar tidal field, in analogy with the linear galaxy bias, $\delta_g(\eta, \mathbf{k}) = b(\eta)\delta_m(\eta, \mathbf{k})$. Ref. [73] proposes an ansatz that the effect of gravitational waves is also imprinted into the shape of galaxies at linear order,

$$\gamma_{AB}^{\text{GW}}(\eta, \mathbf{k}) = b_t^{\text{GW}}(\eta, k)t_{AB}(\eta, \mathbf{k}), \quad (4.1)$$

and the total shape field of galaxies is expressed as the sum of the scalar and tensor contributions [73–75]

$$\gamma_{AB}(\eta, \mathbf{k}) = \gamma_{AB}^S(\eta, \mathbf{k}) + \gamma_{AB}^{\text{GW}}(\eta, \mathbf{k}) = b_K^S(\eta)s_{AB}(\eta, \mathbf{k}) + b_t^{\text{GW}}(\eta, k)t_{AB}(\eta, \mathbf{k}). \quad (4.2)$$

The linear shape bias for GWs, b_t^{GW} , is not independent of b_K^S . By matching the second-order density induced by scalar and tensor tidal fields, Ref. [73] introduced the ansatz for the relation between them as $b_t^{\text{GW}}(\eta, k) \propto \alpha(\eta, k)b_K^S(\eta)$ (see Refs. [73, 75] for the explicit form of α). This relation has been tested and confirmed using N -body simulations [75]. Using this relation, we can immediately obtain the power spectrum of projected shape from that of the projected tidal field derived in section 3.1. By taking the divergence and curl operation on the galaxy shape, we can obtain $\gamma_A(\eta, \mathbf{x})$, $*\gamma_A(\eta, \mathbf{x})$ and $*\gamma(\eta, \mathbf{x})$ as $\gamma_A = \partial^B \gamma_{BA}$, $*\gamma_A = \epsilon^{BC} \partial_B \gamma_{CA}$, and $*\gamma = \partial^A *\gamma_A$, respectively. Note again that all these quantities are trace-free and the superscript T is omitted. Since they are linearly related to the projected tidal force field, measuring the auto-correlation of $*\gamma$ enables us to extract GW signals. The cross-correlation of the divergence (γ_A) and curl ($*\gamma_A$) of the projected shape field becomes nonzero only if there exists parity-violating signals.

In this paper we considered various types of correlations of the projected tidal force field in three dimensions, which are observable in spectroscopic galaxy surveys. The positions of galaxies are sampled by their redshifts in such galaxy surveys, and thus affected by redshift-space distortions (RSD) [91]. We assumed the validity of linear theory. While the shape field is not affected by RSD on linear scales, it is on nonlinear scales [92, 93]. Furthermore, on such small scales, the linear relation between the tidal field and galaxy shapes needs to be modulated. We thus need to consider the higher-order nonlinear shape bias effect [e.g., 94]. To place quantitative constraints on the amplitude of GWs and the chiral parameter, we need to consider more accurate models. It is left to our future work.

Acknowledgments

We thank Kazuyuki Akitsu, Atsushi Taruya and Toshiki Kurita for fruitful discussion. We also thank the workshop ‘*Large-scale Parity Violation Workshop*’ held at Academia Sinica Institute of Astronomy and Astrophysics (ASIAA) during which this project was advanced. T.O. acknowledges support from the Ministry of Science and Technology of Taiwan under grants No. NSTC 112-2112-M-001-034- and No. NSTC 113-2112-M-001-011- and the Career Development Award, Academia Sinica (AS-CDA-108-M02) for the period of 2019-2023. This work is also supported in part by JSPS KAKENHI Nos. JP20H05853 and JP24K00624.

A Relation to E/B-mode decomposition

We describe how our formalism is related to that of the E/B-modes shown in Ref. [75–77]. The 2-dimensional metric perpendicular to the line of sight, g_{AB} , is given by

$$g_{AB} = \hat{x}_A \hat{x}_B + \hat{y}_A \hat{y}_B. \quad (\text{A.1})$$

We also define the polarization tensors of the E- and B-modes, respectively as

$$e_{AB}^{(E)} = \frac{1}{\sqrt{2}} (\hat{x}_A \hat{x}_B - \hat{y}_A \hat{y}_B), \quad e_{AB}^{(B)} = \frac{1}{\sqrt{2}} (\hat{x}_A \hat{y}_B + \hat{y}_A \hat{x}_B). \quad (\text{A.2})$$

These E- and B-modes are related to the R- and L-mode polarization tensors used in the main text as

$$[e_{AB}^{(R,L)}]^T = e_{AB}^{(R,L)} - \frac{1}{2} (g^{CD} e_{CD}^{(R,L)}) \delta_{AB} = \frac{1}{\sqrt{2}} \left[\frac{1 + \mu_k^2}{2} e_{AB}^{(E)} \pm i \mu_k e_{AB}^{(B)} \right], \quad (\text{A.3})$$

where μ_k is the directional cosine of the wavevector \mathbf{k} with respect to the line of sight, and the superscript T stands for the quantity with the trace subtracted. Then the traceless $[h_{AB}]^T$ reads:

$$\begin{aligned} [h_{AB}]^T &= h_{(R)} [e_{AB}^{(R)}]^T + h_{(L)} [e_{AB}^{(L)}]^T \\ &= \frac{1}{\sqrt{2}} \left[\frac{1 + \mu_k^2}{2} e_{AB}^{(E)} + i \mu_k e_{AB}^{(B)} \right] h_{(R)} - \frac{1}{\sqrt{2}} \left[\frac{1 + \mu_k^2}{2} e_{AB}^{(E)} - i \mu_k e_{AB}^{(B)} \right] h_{(L)} \end{aligned} \quad (\text{A.4})$$

Thus, the E- and B-modes of the projected GWs are expressed as

$$h_{(E)} = h_{AB} e_{(E)}^{AB} = \frac{1}{\sqrt{2}} \frac{1 + \mu_k^2}{2} (h_{(R)} + h_{(L)}), \quad (\text{A.5})$$

$$h_{(B)} = h_{AB} e_{(B)}^{AB} = \frac{i}{\sqrt{2}} \mu_k (h_{(R)} - h_{(L)}). \quad (\text{A.6})$$

Finally, the power spectra P_{XY} defined by $\langle h^{(X)}(\eta, \mathbf{k}') h^{(Y)}(\eta', \mathbf{k}') \rangle = (2\pi)^3 \delta_D(\mathbf{k} + \mathbf{k}') P_{XY}(\eta, \eta', \mathbf{k})$, where $XY = \{EE, BB, EB\}$, are respectively given by

$$P_{EE}(\eta, \eta', \mathbf{k}) = \frac{1}{8} (1 + \mu_k^2)^2 (P_{(R)} + P_{(L)}) = \frac{1}{8} (1 + \mu_k^2)^2 P_h(\eta, \eta', k), \quad (\text{A.7})$$

$$P_{BB}(\eta, \eta', \mathbf{k}) = \frac{1}{4} \mu_k^2 (P_{(R)} + P_{(L)}) = \frac{1}{4} \mu_k^2 P_h(\eta, \eta', k), \quad (\text{A.8})$$

$$P_{EB}(\eta, \eta', \mathbf{k}) = \frac{i}{4} \mu_k (1 + \mu_k^2) (P_{(R)} - P_{(L)}) = \frac{i}{4} \mu_k (1 + \mu_k^2) \chi(k) P_h(\eta, \eta', k), \quad (\text{A.9})$$

These are the power spectra already given in Refs. [75–77].

B Power spectra of projected field before subtracting the trace

The tidal force field corresponding to observables is the projected field with the trace part subtracted, and the expressions of the power spectra were shown in section 3. In this appendix, for completeness, we present the power spectra of the projected field before the trace part is subtracted, though they may not be direct observables.

The power spectrum of the projected scalar tidal field is given by

$$\langle s^{AB}(\eta, \mathbf{k}) s_{AB}(\eta', \mathbf{k}') \rangle = k^4 (2\pi)^3 \delta_D(\mathbf{k} + \mathbf{k}') (1 - \mu_k^2)^2 P_\psi(\eta, \eta', k). \quad (\text{B.1})$$

By comparing this with equation (3.4), one can see that the shape of the power spectrum for the projected scalar tidal field is unchanged, $\langle s^{AB} s_{AB} \rangle = 2 \langle s^{T,AB} s_{AB}^T \rangle$. The power spectrum of the projected tensor tidal field without subtracting the trace part is given by

$$\langle h^{AB}(\eta, \mathbf{k}) h_{AB}(\eta', \mathbf{k}') \rangle = \frac{1}{4} (2\pi)^3 \delta_D(\mathbf{k} + \mathbf{k}') (1 + \mu_k^2)^2 P_h(\eta, \eta', k). \quad (\text{B.2})$$

The divergence and curl of the projected field before the trace is subtracted are given by equation (3.6). The power spectrum of the divergence is given by

$$\langle s^A(\eta, \mathbf{k}) s_A(\eta', \mathbf{k}') \rangle = (2\pi)^3 \delta_D(\mathbf{k} + \mathbf{k}') k^6 (1 - \mu_k^2)^3 P_\psi(\eta, \eta', k), \quad (\text{B.3})$$

where it is related to that with the trace part subtracted via $\langle s^A s_A \rangle = 4 \langle s^{T,A} s_A^T \rangle$. Since ${}^*s_A = 0$, $\langle {}^*s^A {}^*s_A \rangle = 0$.

The auto-power spectra of the divergence and curl of the projected tidal tensor field are, respectively, given by

$$\langle h^A(\eta, \mathbf{k}) h_A(\eta', \mathbf{k}') \rangle = \frac{k^2}{4} (2\pi)^3 \delta_D(\mathbf{k} + \mathbf{k}') \mu_k^2 (1 - \mu_k^4) P_h(\eta, \eta', k), \quad (\text{B.4})$$

$$\langle {}^*h^A(\eta, \mathbf{k}) {}^*h_A(\eta', \mathbf{k}') \rangle = \frac{k^2}{4} (2\pi)^3 \delta_D(\mathbf{k} + \mathbf{k}') (1 - \mu_k^4) P_h(\eta, \eta', k). \quad (\text{B.5})$$

These two power spectra are related to each other as $\langle h^A h_A \rangle = \mu_k^2 \langle {}^*h^A {}^*h_A \rangle$.

Finally, the two power spectra, which can directly probe a GW signal and parity-violating signals, have the same forms before and after the trace part subtracted:

$$\langle {}^*h^T(\eta, \mathbf{k}) {}^*h^T(\eta', \mathbf{k}') \rangle = \langle {}^*h(\eta, \mathbf{k}) {}^*h(\eta', \mathbf{k}') \rangle, \quad (\text{B.6})$$

$$\langle {}^*h^{T,A}(\eta, \mathbf{k}) h_A^T(\eta', \mathbf{k}') \rangle = \langle {}^*h^A(\eta, \mathbf{k}) h_A(\eta', \mathbf{k}') \rangle. \quad (\text{B.7})$$

C Derivation of power spectra of projected tidal force field

C.1 Power spectra of scalar tidal field

In this appendix, we provide derivations for the formulas of the power spectra of the scalar tidal field presented in section 3. The Fourier component of the projected scalar tidal field with the trace component subtracted, $s_{AB}^T(\eta, \mathbf{x})$, is given by

$$s_{AB}^T(\eta, \mathbf{k}) = \left(-k_A k_B + \frac{1}{2} \delta_{AB} k^C k_C \right) \psi(\eta, \mathbf{k}). \quad (\text{C.1})$$

Thus it is straightforward to obtain the auto-power spectrum (equation (3.4)),

$$\begin{aligned}
& \langle s^{T,AB}(\eta, \mathbf{k}) s_{AB}^T(\eta', \mathbf{k}') \rangle \\
&= \left(-k^A k^B + \frac{1}{2} \delta^{AB} k_C k^C \right) \left(-k'_A k'_B + \frac{1}{2} \delta_{AB} k'_D k'^D \right) \langle \psi(\eta, \mathbf{k}) \psi(\eta', \mathbf{k}') \rangle \\
&= k^4 \left[(1 - \mu_k^2)^2 - (1 - \mu_k^2)^2 + \frac{1}{2} (1 - \mu_k^2)^2 \right] \langle \psi(\eta, \mathbf{k}) \psi(\eta', \mathbf{k}') \rangle \\
&= \frac{1}{2} (2\pi)^3 \delta_D(\mathbf{k} + \mathbf{k}') k^4 (1 - \mu_k^2)^2 P_\psi(\eta, \eta', k). \tag{C.2}
\end{aligned}$$

For the divergence and curl of the projected scalar tidal field with the trace part subtracted, we have from equation (C.1), respectively,

$$s_A^T(\eta, \mathbf{k}) = -\frac{i}{2} k^B k_B k_A \psi(\eta, \mathbf{k}), \quad {}^*s_A^T(\eta, \mathbf{k}) = \frac{i}{2} \epsilon^{CA} k^B k_B k_C \psi(\eta, \mathbf{k}). \tag{C.3}$$

The auto-power spectrum of the latter, shown in equation (3.10), is obtained as

$$\begin{aligned}
& \langle {}^*s^{T,A}(\eta, \mathbf{k}) {}^*s_A^T(\eta', \mathbf{k}') \rangle \\
&= -\frac{1}{4} (\epsilon^{CA} k^B k_B k_C) (\epsilon_{EA} k'^D k'_D k'^E) \langle \psi(\eta, \mathbf{k}) \psi(\eta', \mathbf{k}') \rangle \\
&= -\frac{1}{4} (\delta_E^C \delta_A^E - \delta_A^C \delta_A^E) (k^B k_B) (k'^D k'_D) k_C k'_E \langle \psi(\eta, \mathbf{k}) \psi(\eta', \mathbf{k}') \rangle \\
&= \frac{1}{4} (2\pi)^3 \delta_D(\mathbf{k} + \mathbf{k}') k^6 (1 - \mu_k^2)^3 P_\psi(\eta, \eta', k). \tag{C.4}
\end{aligned}$$

The auto-power spectrum of s_A^T can be derived similarly and it is easy to show that they are equivalent, $\langle s^{T,A}(\eta, \mathbf{k}) s_A^T(\eta', \mathbf{k}') \rangle = \langle {}^*s^{T,A}(\eta, \mathbf{k}) {}^*s_A^T(\eta', \mathbf{k}') \rangle$.

Note that when we perform the calculations for the scalar tidal field without subtracting the trace part, we can instead obtain equations (B.1) and (B.3).

C.2 Power spectra of tensor tidal field

Here, we provide derivations for the formulas of the power spectra of the tensor tidal field presented in section 3. Throughout this appendix, we repeatedly use the relation,

$$h_z^z = - \sum_{\lambda=R,L} e_{AA}^{(\lambda)} h_{(\lambda)} = -\frac{1}{2} (1 - \mu_k^2) \sum_{\lambda=R,L} h_{(\lambda)}. \tag{C.5}$$

Since GWs are traceless in three dimensions, $h^A_A = h^x_x + h^y_y = -h^z_z$.

The traceless part of the projected GWs is given by

$$h_{AB}^T(\eta, \mathbf{k}) = h_{AB}(\eta, \mathbf{k}) + \frac{1}{2} \delta_{AB} h_z^z(\eta, \mathbf{k}). \tag{C.6}$$

The temporal auto correlation function in Fourier space is obtained as

$$\begin{aligned}
& \langle h^{T,AB}(\eta, \mathbf{k}) h_{AB}^T(\eta', \mathbf{k}') \rangle \\
&= \left\langle \left[h^{AB}(\eta, \mathbf{k}) + \frac{1}{2} \delta^{AB} h_z^z(\eta, \mathbf{k}) \right] \left[h_{AB}(\eta', \mathbf{k}') + \frac{1}{2} \delta_{AB} h_z^z(\eta', \mathbf{k}') \right] \right\rangle \\
&= \langle h^{AB}(\eta, \mathbf{k}) h_{AB}(\eta', \mathbf{k}') \rangle + \langle h^A_A(\eta, \mathbf{k}) h_z^z(\eta', \mathbf{k}') \rangle + \frac{1}{2} \langle h_z^z(\eta, \mathbf{k}) h_z^z(\eta', \mathbf{k}') \rangle \\
&= \frac{1}{8} (2\pi)^3 \delta_D(\mathbf{k} + \mathbf{k}') (1 + 6\mu_k^2 + \mu_k^4) P_h(\eta, \eta', k), \tag{C.7}
\end{aligned}$$

which gives equation (3.5). Here we used the relation, $\sum_{\lambda=R,L} e_{(\lambda)}^{AB} \bar{e}_{AB}^{(\lambda)} = (1 + \mu_k^2)^2/2$.

In the rest of this appendix, we present derivations of the power spectra of divergence and curl of the projected tidal tensor field given in section 3.2. Let us first show the explicit form of the divergence and curl of the projected tidal tensor field, h_A and $*h_A$, and the divergence of the curl of the field, $*h$. We start by showing the expressions before subtracting the trace part. They are given by

$$\begin{aligned} h_A(\eta, \mathbf{k}) &= ik^B h_{BA}(\eta, \mathbf{k}) = ik^B \sum_{\lambda=R,L} e_{BA}^{(\lambda)}(\hat{\mathbf{k}}) h_{(\lambda)}(\eta, \mathbf{k}) \\ &= -\frac{k}{2} \cos \theta_k \sin \theta_k [(h_{(R)} - h_{(L)}) \hat{x}_A + i \cos \theta_k (h_{(R)} + h_{(L)}) \hat{y}_A], \end{aligned} \quad (\text{C.8})$$

$$\begin{aligned} *h_A(\eta, \mathbf{k}) &= ik_B \epsilon^{BC} h_{CA}(\eta, \mathbf{k}) = ik_B \epsilon^{BC} \sum_{\lambda=R,L} e_{CA}^{(\lambda)}(\hat{\mathbf{k}}) h_{(\lambda)}(\eta, \mathbf{k}) \\ &= \frac{k}{2} \sin \theta_k [\cos \theta_k (h_{(R)} - h_{(L)}) \hat{y}_A - i (h_{(R)} + h_{(L)}) \hat{x}_A], \end{aligned} \quad (\text{C.9})$$

$$*h(\eta, \mathbf{k}) = ik^A *h_A(\eta, \mathbf{k}) = \frac{i}{2} k^2 (1 - \mu_k^2) \mu_k (h_{(R)} - h_{(L)}). \quad (\text{C.10})$$

For the second equality in equation (C.8), we used the relations:

$$\begin{aligned} \hat{k}^B e_{BA}^{(+)} &= \frac{1}{\sqrt{2}} \hat{k}^B (e_B^{(1)} e_A^{(1)} - e_B^{(2)} e_A^{(2)}) = -\frac{1}{\sqrt{2}} \cos^2 \theta_k \sin \theta_k \hat{y}_A, \\ \hat{k}^B e_{BA}^{(\times)} &= \frac{1}{\sqrt{2}} \hat{k}^B (e_B^{(1)} e_A^{(2)} + e_B^{(2)} e_A^{(1)}) = \frac{1}{\sqrt{2}} \cos \theta_k \sin \theta_k \hat{x}_A, \end{aligned}$$

and similarly for the second equality in equation (C.9), we used the relations:

$$\hat{k}_B \epsilon^{BC} e_{CA}^{(+)} = -\frac{1}{\sqrt{2}} \sin \theta_k \hat{x}_A, \quad \hat{k}_B \epsilon^{BC} e_{CA}^{(\times)} = -\frac{1}{\sqrt{2}} \cos \theta_k \sin \theta_k \hat{y}_A.$$

Next we show the divergence and curl of the projected tidal tensor field with the trace part subtracted, namely, h_A^T , $*h_A^T$ and $*h^T$. From equation (C.6), we have

$$\begin{aligned} h_A^T(\eta, \mathbf{k}) &= h_A(\eta, \mathbf{k}) + \frac{i}{2} k_A h^z{}_z(\eta, \mathbf{k}), \\ &= -\frac{k}{2} \sin \theta_k \left[\cos \theta_k (h_{(R)} - h_{(L)}) \hat{x}_A + \frac{i}{2} (1 + \cos^2 \theta_k) (h_{(R)} + h_{(L)}) \hat{y}_A \right], \end{aligned} \quad (\text{C.11})$$

$$\begin{aligned} *h_A^T(\eta, \mathbf{k}) &= *h_A(\eta, \mathbf{k}) + \frac{i}{2} k^B \epsilon_{BA} h^z{}_z(\eta, \mathbf{k}) \\ &= \frac{k}{2} \sin \theta_k \left[\cos \theta_k (h_{(R)} - h_{(L)}) \hat{y}_A - \frac{i}{2} (1 + \cos^2 \theta_k) (h_{(R)} + h_{(L)}) \hat{x}_A \right] \end{aligned} \quad (\text{C.12})$$

$$*h^T(\eta, \mathbf{k}) = ik^A *h_A^T(\eta, \mathbf{k}) = *h(\eta, \mathbf{k}). \quad (\text{C.13})$$

From the above, one can derive the temporal correlation functions of the various quantities:

$$\begin{aligned}
\langle h^{T,A}(\eta, \mathbf{k}) h_A^T(\eta', \mathbf{k}') \rangle &= \left\langle \left(h^A(\eta, \mathbf{k}) + \frac{i}{2} k^A h_z^z(\eta, \mathbf{k}) \right) \left(h_A(\eta', \mathbf{k}') + \frac{i}{2} k_A h_z^z(\eta', \mathbf{k}') \right) \right\rangle \\
&= \frac{1}{4} (2\pi)^3 \delta_D(\mathbf{k} + \mathbf{k}') \sin^2 \theta_k \left[\cos^2 \theta_k + \frac{1}{4} (1 + \cos^2 \theta_k)^2 \right] P_h(\eta, \eta', k) \\
&= \frac{1}{16} (2\pi)^3 \delta_D(\mathbf{k} + \mathbf{k}') k^2 (1 - \mu_k^2) (1 + 6\mu_k^2 + \mu_k^4) P_h(\eta, \eta', k), \quad (\text{C.14})
\end{aligned}$$

$$\begin{aligned}
\langle {}^* h^T(\eta, \mathbf{k}) {}^* h^T(\eta', \mathbf{k}') \rangle &= \langle (i k^A {}^* h_A(\eta, \mathbf{k})) (i k^B {}^* h_B(\eta', \mathbf{k}')) \rangle \\
&= \frac{1}{4} (2\pi)^3 \delta_D(\mathbf{k} + \mathbf{k}') k^4 \mu_k^2 (1 - \mu_k^2)^2 P_h(\eta, \eta', k), \quad (\text{C.15})
\end{aligned}$$

$$\begin{aligned}
\langle {}^* h^{T,A}(\eta, \mathbf{k}) h_A^T(\eta', \mathbf{k}') \rangle &= \left\langle \left({}^* h^A(\eta, \mathbf{k}) + \frac{i}{2} k_B \epsilon^{BA} h_z^z(\eta, \mathbf{k}) \right) \left(h_A(\eta', \mathbf{k}') + \frac{i}{2} k_A h_z^z(\eta', \mathbf{k}') \right) \right\rangle \\
&= \frac{i}{4} (2\pi)^3 \delta_D(\mathbf{k} + \mathbf{k}') k^2 \cos \theta_k \sin^2 \theta_k (\cos^2 \theta_k + 1) P_h(\eta, \eta', k) \\
&= \frac{i}{4} (2\pi)^3 \delta_D(\mathbf{k} + \mathbf{k}') k^2 \mu_k (1 - \mu_k^4) P_h(\eta, \eta', k), \quad (\text{C.16})
\end{aligned}$$

which respectively give equations (3.11), (3.13) and (3.14).

References

- [1] A.A. Starobinskiĭ, *Spectrum of relict gravitational radiation and the early state of the universe*, *Soviet Journal of Experimental and Theoretical Physics Letters* **30** (1979) 682.
- [2] M. Zaldarriaga and U. Seljak, *All-sky analysis of polarization in the microwave background*, *Phys. Rev. D* **55** (1997) 1830 [[astro-ph/9609170](#)].
- [3] M. Kamionkowski, A. Kosowsky and A. Stebbins, *Statistics of cosmic microwave background polarization*, *Phys. Rev. D* **55** (1997) 7368 [[astro-ph/9611125](#)].
- [4] J. Luo, L.-S. Chen, H.-Z. Duan, Y.-G. Gong, S. Hu, J. Ji et al., *TianQin: a space-borne gravitational wave detector*, *Classical and Quantum Gravity* **33** (2016) 035010 [[1512.02076](#)].
- [5] P. Amaro-Seoane, H. Audley, S. Babak, J. Baker, E. Barausse, P. Bender et al., *Laser Interferometer Space Antenna*, *arXiv e-prints* (2017) [arXiv:1702.00786](#) [[1702.00786](#)].
- [6] B.P. Abbott, R. Abbott, T.D. Abbott, M.R. Abernathy, F. Acernese, K. Ackley et al., *Prospects for observing and localizing gravitational-wave transients with Advanced LIGO, Advanced Virgo and KAGRA*, *Living Reviews in Relativity* **21** (2018) 3 [[1304.0670](#)].
- [7] S. Kawamura, M. Ando, N. Seto, S. Sato, M. Musha, I. Kawano et al., *Current status of space gravitational wave antenna DECIGO and B-DECIGO*, *Progress of Theoretical and Experimental Physics* **2021** (2021) 05A105 [[2006.13545](#)].
- [8] G. Agazie, A. Anumarlapudi, A.M. Archibald, Z. Arzoumanian, P.T. Baker, B. Bécsy et al., *The NANOGrav 15 yr Data Set: Evidence for a Gravitational-wave Background*, *Astrophys. J. Lett.* **951** (2023) L8 [[2306.16213](#)].
- [9] EPTA Collaboration, InPTA Collaboration, J. Antoniadis, P. Arumugam, S. Arumugam, S. Babak et al., *The second data release from the European Pulsar Timing Array. III. Search for gravitational wave signals*, *Astron. Astrophys.* **678** (2023) A50 [[2306.16214](#)].

- [10] H. Xu, S. Chen, Y. Guo, J. Jiang, B. Wang, J. Xu et al., *Searching for the Nano-Hertz Stochastic Gravitational Wave Background with the Chinese Pulsar Timing Array Data Release I*, *Research in Astronomy and Astrophysics* **23** (2023) 075024 [2306.16216].
- [11] N. Kaiser and A. Jaffe, *Bending of Light by Gravity Waves*, *Astrophys. J.* **484** (1997) 545 [astro-ph/9609043].
- [12] S. Dodelson, E. Rozo and A. Stebbins, *Primordial Gravity Waves and Weak Lensing*, *Phys. Rev. Lett.* **91** (2003) 021301 [astro-ph/0301177].
- [13] A. Cooray, M. Kamionkowski and R.R. Caldwell, *Cosmic shear of the microwave background: The curl diagnostic*, *Phys. Rev. D* **71** (2005) 123527 [astro-ph/0503002].
- [14] J. Yoo, A.L. Fitzpatrick and M. Zaldarriaga, *New perspective on galaxy clustering as a cosmological probe: General relativistic effects*, *Phys. Rev. D* **80** (2009) 083514 [0907.0707].
- [15] K.W. Masui and U.-L. Pen, *Primordial Gravity Wave Fossils and Their Use in Testing Inflation*, *Phys. Rev. Lett.* **105** (2010) 161302 [1006.4181].
- [16] S. Dodelson, *Cross-correlating probes of primordial gravitational waves*, *Phys. Rev. D* **82** (2010) 023522 [1001.5012].
- [17] D. Jeong and F. Schmidt, *Large-scale structure with gravitational waves. I. Galaxy clustering*, *Phys. Rev. D* **86** (2012) 083512 [1205.1512].
- [18] F. Schmidt and D. Jeong, *Large-scale structure with gravitational waves. II. Shear*, *Phys. Rev. D* **86** (2012) 083513 [1205.1514].
- [19] F. Schmidt and D. Jeong, *Cosmic rulers*, *Phys. Rev. D* **86** (2012) 083527 [1204.3625].
- [20] N.E. Chisari, C. Dvorkin and F. Schmidt, *Can weak lensing surveys confirm BICEP2?*, *Phys. Rev. D* **90** (2014) 043527 [1406.4871].
- [21] Y. Minami and E. Komatsu, *New Extraction of the Cosmic Birefringence from the Planck 2018 Polarization Data*, *Phys. Rev. Lett.* **125** (2020) 221301 [2011.11254].
- [22] J.R. Eskilt and E. Komatsu, *Improved constraints on cosmic birefringence from the WMAP and Planck cosmic microwave background polarization data*, *Phys. Rev. D* **106** (2022) 063503 [2205.13962].
- [23] P. Diego-Palazuelos, J.R. Eskilt, Y. Minami, M. Tristram, R.M. Sullivan, A.J. Banday et al., *Cosmic Birefringence from the Planck Data Release 4*, *Phys. Rev. Lett.* **128** (2022) 091302 [2201.07682].
- [24] M. Iye, K.-i. Tadaki and H. Fukumoto, *Spin Parity of Spiral Galaxies. I. Corroborative Evidence for Trailing Spirals*, *Astrophys. J.* **886** (2019) 133 [1910.10926].
- [25] H.-R. Yu, P. Motloch, U.-L. Pen, Y. Yu, H. Wang, H. Mo et al., *Probing Primordial Chirality with Galaxy Spins*, *Phys. Rev. Lett.* **124** (2020) 101302 [1904.01029].
- [26] P. Motloch, H.-R. Yu, U.-L. Pen and Y. Xie, *An observed correlation between galaxy spins and initial conditions*, *Nature Astronomy* **5** (2021) 283 [2003.04800].
- [27] P. Motloch, U.-L. Pen and H.-R. Yu, *Observational search for primordial chirality violations using galaxy angular momenta*, *Phys. Rev. D* **105** (2022) 083512 [2111.12590].
- [28] J. Shim, U.-L. Pen, H.-R. Yu and T. Okumura, *Probing vector chirality in the early Universe*, *arXiv e-prints* (2024) arXiv:2406.06080 [2406.06080].
- [29] O.H.E. Philcox, *Probing parity violation with the four-point correlation function of BOSS galaxies*, *Phys. Rev. D* **106** (2022) 063501 [2206.04227].
- [30] J. Hou, Z. Slepian and R.N. Cahn, *Measurement of parity-odd modes in the large-scale 4-point correlation function of Sloan Digital Sky Survey Baryon Oscillation Spectroscopic Survey twelfth data release CMASS and LOWZ galaxies*, *Mon. Not. Roy. Astron. Soc.* **522** (2023)

- 5701 [2206.03625].
- [31] O.H.E. Philcox, *Do the CMB Temperature Fluctuations Conserve Parity?*, *Phys. Rev. Lett.* **131** (2023) 181001 [2303.12106].
 - [32] O.H.E. Philcox and M. Shiraishi, *Testing parity symmetry with the polarized cosmic microwave background*, *Phys. Rev. D* **109** (2024) 083514 [2308.03831].
 - [33] A. Lue, L. Wang and M. Kamionkowski, *Cosmological Signature of New Parity-Violating Interactions*, *Phys. Rev. Lett.* **83** (1999) 1506 [astro-ph/9812088].
 - [34] R. Jackiw and S.Y. Pi, *Chern-Simons modification of general relativity*, *Phys. Rev. D* **68** (2003) 104012 [gr-qc/0308071].
 - [35] N. Seto, *Prospects for Direct Detection of the Circular Polarization of the Gravitational-Wave Background*, *Phys. Rev. Lett.* **97** (2006) 151101 [astro-ph/0609504].
 - [36] S. Saito, K. Ichiki and A. Taruya, *Probing polarization states of primordial gravitational waves with CMB anisotropies*, *JCAP* **09** (2007) 002 [0705.3701].
 - [37] N. Seto and A. Taruya, *Measuring a Parity-Violation Signature in the Early Universe via Ground-Based Laser Interferometers*, *Phys. Rev. Lett.* **99** (2007) 121101 [0707.0535].
 - [38] N. Seto and A. Taruya, *Polarization analysis of gravitational-wave backgrounds from the correlation signals of ground-based interferometers: Measuring a circular-polarization mode*, *Phys. Rev. D* **77** (2008) 103001 [0801.4185].
 - [39] M. Satoh, S. Kanno and J. Soda, *Circular polarization of primordial gravitational waves in string-inspired inflationary cosmology*, *Phys. Rev. D* **77** (2008) 023526 [0706.3585].
 - [40] D. Jeong and M. Kamionkowski, *Clustering Fossils from the Early Universe*, *Phys. Rev. Lett.* **108** (2012) 251301 [1203.0302].
 - [41] A. Maleknejad, M.M. Sheikh-Jabbari and J. Soda, *Gauge fields and inflation*, *Phys. Rept.* **528** (2013) 161 [1212.2921].
 - [42] K.W. Masui, U.-L. Pen and N. Turok, *Two- and Three-Dimensional Probes of Parity in Primordial Gravity Waves*, *Phys. Rev. Lett.* **118** (2017) 221301 [1702.06552].
 - [43] M. Bastero-Gil and A.T. Manso, *Parity violating gravitational waves at the end of inflation*, *JCAP* **08** (2023) 001 [2209.15572].
 - [44] E. Komatsu, *New physics from the polarized light of the cosmic microwave background*, *Nature Reviews Physics* **4** (2022) 452 [2202.13919].
 - [45] Q. Liang, M.-X. Lin, M. Trodden and S.S.C. Wong, *Probing parity violation in the stochastic gravitational wave background with astrometry*, *Phys. Rev. D* **109** (2024) 083028 [2309.16666].
 - [46] J. Lee and U.-L. Pen, *Cosmic Shear from Galaxy Spins*, *Astrophys. J. Lett.* **532** (2000) L5 [astro-ph/9911328].
 - [47] P. Catelan, M. Kamionkowski and R.D. Blandford, *Intrinsic and extrinsic galaxy alignment*, *Mon. Not. Roy. Astron. Soc.* **320** (2001) L7 [astro-ph/0005470].
 - [48] R.G. Crittenden, P. Natarajan, U.-L. Pen and T. Theuns, *Spin-induced Galaxy Alignments and Their Implications for Weak-Lensing Measurements*, *Astrophys. J.* **559** (2001) 552 [astro-ph/0009052].
 - [49] C.M. Hirata and U. Seljak, *Intrinsic alignment-lensing interference as a contaminant of cosmic shear*, *Phys. Rev. D* **70** (2004) 063526 [astro-ph/0406275].
 - [50] T. Okumura, Y.P. Jing and C. Li, *Intrinsic Ellipticity Correlation of SDSS Luminous Red Galaxies and Misalignment with Their Host Dark Matter Halos*, *Astrophys. J.* **694** (2009) 214 [0809.3790].

- [51] T. Okumura and Y.P. Jing, *The Gravitational Shear-Intrinsic Ellipticity Correlation Functions of Luminous Red Galaxies in Observation and in the Λ CDM Model*, *Astrophys. J. Lett.* **694** (2009) L83 [0812.2935].
- [52] J. Blazek, M. McQuinn and U. Seljak, *Testing the tidal alignment model of galaxy intrinsic alignment*, *JCAP* **5** (2011) 10 [1101.4017].
- [53] N.E. Chisari and C. Dvorkin, *Cosmological information in the intrinsic alignments of luminous red galaxies*, *JCAP* **12** (2013) 029 [1308.5972].
- [54] J. Lee, S. Ryu and M. Baldi, *Disentangling Modified Gravity and Massive Neutrinos with Intrinsic Shape Alignments of Massive Halos*, *Astrophys. J.* **945** (2023) 15 [2206.03406].
- [55] F. Schmidt, N.E. Chisari and C. Dvorkin, *Imprint of inflation on galaxy shape correlations*, *JCAP* **10** (2015) 032 [1506.02671].
- [56] N.E. Chisari, C. Dvorkin, F. Schmidt and D.N. Spergel, *Multitracing anisotropic non-Gaussianity with galaxy shapes*, *Phys. Rev. D* **94** (2016) 123507 [1607.05232].
- [57] K. Kogai, K. Akitsu, F. Schmidt and Y. Urakawa, *Galaxy imaging surveys as spin-sensitive detector for cosmological colliders*, *JCAP* **03** (2021) 060 [2009.05517].
- [58] T. Okumura, A. Taruya and T. Nishimichi, *Intrinsic alignment statistics of density and velocity fields at large scales: Formulation, modeling, and baryon acoustic oscillation features*, *Phys. Rev. D* **100** (2019) 103507.
- [59] T. Okumura and A. Taruya, *Anisotropies of galaxy ellipticity correlations in real and redshift space: angular dependence in linear tidal alignment model*, *Mon. Not. Roy. Astron. Soc.* **493** (2020) L124 [1912.04118].
- [60] T. Okumura, A. Taruya and T. Nishimichi, *Testing tidal alignment models for anisotropic correlations of halo ellipticities with N-body simulations*, *Mon. Not. Roy. Astron. Soc.* **494** (2020) 694 [2001.05302].
- [61] K. Akitsu, T. Kurita, T. Nishimichi, M. Takada and S. Tanaka, *Imprint of anisotropic primordial non-Gaussianity on halo intrinsic alignments in simulations*, *Phys. Rev. D* **103** (2021) 083508 [2007.03670].
- [62] M. Shiraishi, A. Taruya, T. Okumura and K. Akitsu, *Wide-angle effects on galaxy ellipticity correlations*, *Mon. Not. Roy. Astron. Soc.* **503** (2021) L6 [2012.13290].
- [63] K. Akitsu, Y. Li and T. Okumura, *Cosmological simulation in tides: power spectra, halo shape responses, and shape assembly bias*, *JCAP* **04** (2021) 041 [2011.06584].
- [64] J. Shi, K. Osato, T. Kurita and M. Takada, *An Optimal Estimator of Intrinsic Alignments for Star-forming Galaxies in IllustrisTNG Simulation*, *Astrophys. J.* **917** (2021) 109 [2104.12329].
- [65] T. Kurita and M. Takada, *Analysis method for 3D power spectrum of projected tensor fields with fast estimator and window convolution modeling: An application to intrinsic alignments*, *Phys. Rev. D* **105** (2022) 123501 [2202.11839].
- [66] A. Taruya and T. Okumura, *Improving Geometric and Dynamical Constraints on Cosmology with Intrinsic Alignments of Galaxies*, *Astrophys. J. Lett.* **891** (2020) L42 [2001.05962].
- [67] T. Okumura and A. Taruya, *Tightening geometric and dynamical constraints on dark energy and gravity: Galaxy clustering, intrinsic alignment, and kinetic Sunyaev-Zel'dovich effect*, *Phys. Rev. D* **106** (2022) 043523 [2110.11127].
- [68] Y.-T. Chuang, T. Okumura and M. Shirasaki, *Distinguishing between Λ CDM and $f(R)$ gravity models using halo ellipticity correlations in simulations*, *Mon. Not. Roy. Astron. Soc.* **515** (2022) 4464 [2111.01417].
- [69] S. Saga, T. Okumura, A. Taruya and T. Inoue, *Relativistic distortions in galaxy*

- density-ellipticity correlations: gravitational redshift and peculiar velocity effects*, *Mon. Not. Roy. Astron. Soc.* **518** (2023) 4976 [2207.03454].
- [70] M. Shiraishi, T. Okumura and K. Akitsu, *Statistical anisotropy in galaxy ellipticity correlations*, *JCAP* **08** (2023) 013 [2303.10890].
- [71] T. Okumura and A. Taruya, *First Constraints on Growth Rate from Redshift-space Ellipticity Correlations of SDSS Galaxies at $0.16 < z < 0.70$* , *Astrophys. J. Lett.* **945** (2023) L30 [2301.06273].
- [72] T. Kurita and M. Takada, *Constraints on anisotropic primordial non-Gaussianity from intrinsic alignments of SDSS-III BOSS galaxies*, *Phys. Rev. D* **108** (2023) 083533 [2302.02925].
- [73] F. Schmidt, E. Pajer and M. Zaldarriaga, *Large-scale structure and gravitational waves. III. Tidal effects*, *Phys. Rev. D* **89** (2014) 083507 [1312.5616].
- [74] M. Biagetti and G. Orlando, *Primordial Gravitational Waves from Galaxy Intrinsic Alignments*, *JCAP* **07** (2020) 005 [2001.05930].
- [75] K. Akitsu, Y. Li and T. Okumura, *Gravitational wave fossils in nonlinear regime: Halo tidal bias and intrinsic alignments from gravitational wave separate universe simulations*, *Phys. Rev. D* **107** (2023) 063531 [2209.06226].
- [76] O.H.E. Philcox, M.J. König, S. Alexander and D.N. Spergel, *What can galaxy shapes tell us about physics beyond the standard model?*, *Phys. Rev. D* **109** (2024) 063541 [2309.08653].
- [77] S. Saga, M. Shiraishi, K. Akitsu and T. Okumura, *Imprints of primordial magnetic fields on intrinsic alignments of galaxies*, *Phys. Rev. D* **109** (2024) 043520 [2312.16316].
- [78] T. Kurita, M. Takada, T. Nishimichi, R. Takahashi, K. Osato and Y. Kobayashi, *Power spectrum of halo intrinsic alignments in simulations*, *Mon. Not. Roy. Astron. Soc.* **501** (2021) 833 [2004.12579].
- [79] T. Matsubara, *Integrated perturbation theory for cosmological tensor fields. III. Projection effects*, *Phys. Rev. D* **110** (2024) 063545 [2304.13304].
- [80] C.W. Misner, K.S. Thorne and J.A. Wheeler, *Gravitation*, W. H. Freeman, San Francisco (1973).
- [81] M. Isi, *Parametrizing gravitational-wave polarizations*, *Classical and Quantum Gravity* **40** (2023) 203001 [2208.03372].
- [82] P. Creminelli, J. Gleyzes, J. Noreña and F. Vernizzi, *Resilience of the Standard Predictions for Primordial Tensor Modes*, *Phys. Rev. Lett.* **113** (2014) 231301 [1407.8439].
- [83] S. Alexander and J. Martin, *Birefringent gravitational waves and the consistency check of inflation*, *Phys. Rev. D* **71** (2005) 063526 [hep-th/0410230].
- [84] M. Maggiore, *Gravitational Waves. Vol. 2: Astrophysics and Cosmology*, Oxford University Press (3, 2018).
- [85] B. Allen, É.É. Flanagan and M.A. Papa, *Is the squeezing of relic gravitational waves produced by inflation detectable?*, *Phys. Rev. D* **61** (1999) 024024 [gr-qc/9906054].
- [86] A. Margalit, C.R. Contaldi and M. Pieroni, *Phase decoherence of gravitational wave backgrounds*, *Phys. Rev. D* **102** (2020) 083506 [2004.01727].
- [87] E.E. Flanagan, *Sensitivity of the Laser Interferometer Gravitational Wave Observatory to a stochastic background, and its dependence on the detector orientations*, *Phys. Rev. D* **48** (1993) 2389 [astro-ph/9305029].
- [88] B. Allen and J.D. Romano, *Detecting a stochastic background of gravitational radiation: Signal processing strategies and sensitivities*, *Phys. Rev. D* **59** (1999) 102001 [gr-qc/9710117].

- [89] J.D. Romano and N.J. Cornish, *Detection methods for stochastic gravitational-wave backgrounds: a unified treatment*, *Living Reviews in Relativity* **20** (2017) 2 [[1608.06889](#)].
- [90] R.W. Hellings and G.S. Downs, *Upper limits on the isotropic gravitational radiation background from pulsar timing analysis.*, *Astrophys. J. Lett.* **265** (1983) L39.
- [91] N. Kaiser, *Clustering in real space and in redshift space*, *Mon. Not. Roy. Astron. Soc.* **227** (1987) 1.
- [92] T. Matsubara, *Integrated perturbation theory for cosmological tensor fields. I. Basic formulation*, *Phys. Rev. D* **110** (2024) 063543 [[2210.10435](#)].
- [93] T. Okumura, A. Taruya, T. Kurita and T. Nishimichi, *Nonlinear redshift space distortion in halo ellipticity correlations: Analytical model and N -body simulations*, *Phys. Rev. D* **109** (2024) 103501 [[2310.07384](#)].
- [94] K. Akitsu, Y. Li and T. Okumura, *Quadratic shape biases in three-dimensional halo intrinsic alignments*, *JCAP* **08** (2023) 068 [[2306.00969](#)].